FLUID COMPRESSIBILITY EFFECTS ON THE DYNAMIC RESPONSE OF HYDROSTATIC JOURNAL BEARINGS

Luis A. San Andres
Mechanical Engineering Department
Texas A&M University
College Station, Texas 77843-3123, U.S.A.

A theoretical analysis for the dynamic performance characteristics of laminar flow, capillar/orifice compensated hydrostatic journal bearings is presented. The analysis considers in detail the effect of fluid compressibility in the bearing recesses. At high frequency excitations beyond a break frequency, the bearing hydrostatic stiffness increases sharply and it is accompanied by a rapid decrease in direct damping. Also, the potential of pneumatic hammer instability (negative damping) at low frequencies is likely to occur in hydrostatic bearing applications handling highly compressible fluids. Useful design criteria to avoid undesirable dynamic operating conditions at low and high frequencies are determined. The effect of fluid recess compressibility is brought into perspective, and found to be of utmost importance on the entire frequency spectrum response and stability characteristics of hydrostatic/hybrid journal bearings.

INTRODUCTION

The dynamic performance of hydrostatic and hybrid journal bearings (HJBs) has been a subject of growing theoretical interest. In the past, conventional applications of HJBs were restricted to support heavy loads at zero or low speeds and also to low operating eccentricities required for precise machine tools. However, industry's expanding demands for higher speed applications and the ability of bearings to support dynamic loads have brought the need to consider and study in detail the dynamic performance of these type of bearings.

Davies and Leonard (1969) first studied the dynamic behavior of HJBs, and derived under restricted conditions closed form solutions for small motions about the concentric position. The limited stability characteristics of hybrid bearings have been confirmed experimentally by Davies and Leonard (1970, 1971), and Leonard and Rowe(1973). M.K. Ghosh (1979) and V.N. Singh(1979) have also presented numerical analyses for the static and dynamic performance characteristics of HJBs. For best dynamic performance, the analyses show that optimum direct damping is attained at low recess pressure ratios and reduced recess to bearing area ratios. Based on the concentric thin land theory, Rowe (1980) presented coefficients for hydrostatic and hydrodynamic stiffness and squeeze damping for capillary, orifice and constant flow control HJBs. The mechanism of whirl instability for hybrid operation is explained, and

NOMENCLATURE

A	$\pi d^2/4$. Orifice area [m^2]
b	Recess circumferential length [m].
c	radial clearance [m]
$C_{XX}, C_{XY}, C_{YX}, C_{YY}$	damping coefficients [Ns/m]
C_d	Orifice discharge coefficient
D	2 R . Bearing diameter [m].
d_o, d_c	Orifice and capillary diameter [m]
f	ω/ω_B. dynamic frequency ratio.
h	$H/c = 1+\Delta\varepsilon_x\cos\theta + \Delta\varepsilon_y\sin\theta$ Dimensionless film thickness.
h_x, h_y	$\cos\theta$, $\sin\theta$
H_r	Recess depth [m].
$K_{XX}, K_{XY}, K_{YX}, K_{YY}$	Stiffness coefficients [N/m]
L, l	Bearing axial width, recess axial length [m].
N	Number of recesses on bearing.
P	Fluid pressure [N/m^2].
P_a, P_s	Ambient and external supply pressures [N/m^2]
p_r	$(P_r-P_a)/(P_s-P_a)$. recess pressure ratio.
q_r	$Q_r\ \mu/c^3(P_s-P_a)$ Dimensionless recess flow rate into film lands
v_o	$\sqrt{2(P_s-P_r)/\rho}$. Fluid speed through orifice [m/s].
v_{so}	$\sqrt{1/(\beta\rho)}$. Orifice Fluid speed at sonic conditions [m/s]
v_{sc}	$\sqrt{A_c/(\beta\ 8\pi\mu l_c)}$. Capillar fluid speed at sonic conditions
V_r, V_s	$(H_r+H)lb+V_s$ Total recess volume, volume of orifice supply line [m^3].
$\{X,Y\}$	Inertial coordinate system.
z	restrictor control parameter.
α_c	reduced damping factor due to compressibility, eqn. (14)
β	Fluid compressibility factor [m^2/N].

δ_o	$Ao\ \mu\sqrt{2}/c^3/\sqrt{\rho(Ps-Pa)}$ Design Orifice parameter.
δ_c	$A_c^2/(8\pi\ l_c\ c^3)$. Design capillary parameter.
λ_1	$\mu\omega A_r/c^2(Ps-Pa)$ Recess frequency parameter
λ_2	$V_r\beta(Ps-Pa)/clb$. Compressibility parameter
Λ	$\mu\Omega R^2/c^2(Ps-Pa)$ Rotational speed parameter.
σ	$\mu\omega R^2/c^2(Ps-Pa)$ Frequency parameter at film lands.
ω	Excitation or whirling frequency [1/sec]
ω_B	Break frequency [1/s], eqn. (15).
Ω	Rotational speed of journal [1/s]
ϕ	$K_{xy}/\Omega C_{xx}$. Whirl frequency ratio.
$\Delta\varepsilon_x$, $\Delta\varepsilon_y$	Dimensionless perturbed eccentricities
$\delta\Theta, \delta\phi$	$2\pi/N$; b/R
$\Delta\Theta$, $\Delta\Xi$	$\delta\Theta-\delta\phi$; (L-l)/D
τ	ωt Dimensionless time coordinate
Θ, Ξ	(x,y)/R. Dimesionless circumferential and axial coordinate
γ	$\frac{2\Delta\Xi L}{\delta\Theta\ \Delta\Theta\ D}$ Circumferential flow factor

Subscripts:

o	refers to zeroth order solution or no compressibility solution.
r	refers to bearing recesses
α	refers to first order solution

Superscripts:

n	refers to n-th recess

it is shown that the whirl frequency ratio is equal to 0.5. Nonetheless, the introduction of hydrostatic stiffness into the rotor-bearing system raises the frequency of whirl onset.

Rohde and Ezzat (1976) presented an analysis which accounts for the lubricant compressibility in the bearing recesses and supply line. The results, also supported by the analysis of Ghosh and Viswanath (1987) and Ghosh et al. (1989), show that when the journal is subjected to high frequency excitations the bearing stiffness and damping characteristics can change drastically. The behavior is determined by a "break" frequency beyond which the bearing direct stiffness increases sharply and it is accompanied by a rapid decrease in direct damping. The analyses cited are based on full numerical solutions to the Reynolds equations, and thus, their results can not be easily used in practice.

The present work introduces a theoretical analysis for the dynamic performance characteristics of capillar/orifice compensated centered hydrostatic journal bearings. The analysis considers in detail the effect of fluid recess compressibility. Useful design criteria to avoid undesirable dynamic operating conditions at low and high frequencies are determined. Conditions to avoid complete loss of damping at small frequencies are also presented.
The relevance of the analysis is immediately recognized since the performance characteristics of HJBs are relatively independent of the static journal center displacement for small to moderate values of the eccentricity vector.

ANALYSIS

The geometry of a hydrostatic bearing and reference coordinate systems are shown in Figure 1. A lubricant at external pressure P_s is supplied through either a capillary or orifice to each recess, flows into the film lands, and then exits the bearing. The performance characteristics of HJBs are governed by momentum and continuity considerations at the film lands as well as flow continuity through the recesses. The former define the pressure and flow fields over the thin film region, whereas the latter provides values for the pressure in the recesses.

The continuity equation at each recess determines the global flow balance between the flow through the orifice (Q_o) or capillary (Q_c) restrictors, the recess outflow into the film lands (Q_r), and the time change of fluid mass within the recess volume. The recess continuity equation is then given as

$$Q_i = Q_r + \frac{\partial V_r}{\partial t} + V_r \beta \frac{\partial P_r}{\partial t} \qquad (1)$$

where β represents the fluid compressibility factor. The inlet flow (Q_i) through the external restrictor depends on the nature of the control device, i.e.

for orifice:

$$Qi = Qo = Cd \frac{\pi d_o^2}{4} \sqrt{2 (P_s - P_r)/\rho} \qquad (2a)$$

for capillar:

$$Q_i = Q_c = \frac{\pi d_c^4}{128 \mu l_c} (P_s - P_r) \qquad (2b)$$

For small amplitude motions of frequency ω about the concentric position, the land film thickness is described by the real part of the expression:

$$h = H/c = 1 + e^{i\tau} (\Delta\varepsilon_x h_x + \Delta\varepsilon_y h_y) \qquad (3)$$

$$h_x = \cos \theta , \; h_y = \sin \theta$$

$$\tau = \omega t, \quad \Delta\varepsilon_x, \; \Delta\varepsilon_y << 1$$

The film land and recess pressures are expressed as the sum of a zeroth and first order complex fields describing the equilibrium centered position and the perturbed dynamic motion, respectively. Hence, in dimensionless form

$$p = p_o + e^{i\tau} (\Delta\varepsilon_x p_x + \Delta\varepsilon_y p_y) \qquad (4)$$

$$p_r = p_{ro} + e^{i\tau} (\Delta\varepsilon_x p_{rx} + \Delta\varepsilon_y p_{ry})$$

The linear perturbation method used determines the recess continuity equation to be accordingly divided into zeroth and first order expressions as

<u>zeroth order recess continuity equation:</u>

a)capillary: $$\delta_c (1 - p_{ro}) = q_{ro} \qquad (5a)$$

b) orifice: $$\delta_o \sqrt{(1-p_{ro})} = q_{ro} \qquad (5b)$$

and the dimensionless film flow into the lands is given by (Davies, 1969, Rowe, 1980) as

$$q_{ro} = \frac{\delta\theta}{12\Delta\xi} p_{ro} \qquad (6)$$

δ_c and δ_o are the capillary and orifice design parameters that help to determine the restrictor geometry for the desired operating pressure ratio.

<u>first order recess continuity equation at nth recess:</u>

a)capillary: $$-p_{r\alpha}^{\,n} [\delta_c + i \lambda_1 \lambda_2] = q_{r\alpha}^{\,n} \qquad (7a)$$

b)orifice: $$-p_{r\alpha}^{\,n} [\frac{\delta_o^2}{2q_{ro}} + i \lambda_1 \lambda_2] = q_{r\alpha}^{\,n} \qquad (7b)$$

$$\alpha = x,y; \; n=1,2,\ldots,N$$

and $q_{r\alpha}^{\,n}$ is the perturbed land flow on the closure surrounding the nth recess. For laminar flow, the film flow is equal to (Rowe, 1980, SanAndres, 1989a)

$$
\begin{aligned}
q_{r\alpha}^{\,n} = {} & \frac{p_{ro}}{2\Delta\xi}\int_{\theta_n}^{\theta_{n+1}} h_\alpha \, d\theta + \frac{2\delta\theta}{12\Delta\xi}\, p_{r\alpha}^{\,n} && \text{..... hydrostatic axial flow} \\
& + \frac{L/D}{6\ \Delta\theta}\left[\, 2\, p_{r\alpha}^{\,n} - p_{r\alpha}^{\,n+1} - p_{r\alpha}^{\,n-1}\,\right] && \text{..... hydrostatic circ. flow} \\
& + 2\,\frac{L}{D}\,\frac{\Lambda}{2}\, h_\alpha \Big|_{\theta_n}^{\theta_{n+1}} && \text{..... hydrodynamic flow} \\
& + i\,\sigma\,\frac{L}{D}\int_{\theta_n}^{\theta_{n+1}} h_\alpha \, d\theta && \text{..... squeeze film flow}
\end{aligned}
\qquad (8)
$$

$$\theta_n = n\delta\theta$$

Collecting similar terms, equations (7) are reduced to

$$
\begin{aligned}
& \frac{\gamma}{2}\left(\, p_{r\alpha}^{\,n+1} - p_{r\alpha}^{\,n-1}\right) - \left(\, z+1+\gamma + i\,\lambda_1\lambda_2\,\frac{6\Delta\xi}{\delta\theta}\right) p_{r\alpha}^{\,n} = \\
& = \frac{3p_{ro}}{\delta\theta}\int_{\theta_n}^{\theta_{n+1}} h_\alpha \, d\theta + 12\,\frac{L\Delta\xi}{D\delta\theta}\left[\frac{\Lambda}{2}\, h_\alpha \Big|_{\theta_n}^{\theta_{n+1}} + i\,\sigma\int_{\theta_n}^{\theta_{n+1}} h_\alpha \, d\theta\right]
\end{aligned}
\qquad (9)
$$

$$n=1,2,\ldots.\ N$$

where z is a control parameter, first introduced by Rowe (1980), and given as

$$z = z_o = \frac{p_{ro}}{2(1-p_{ro})}\ ;\ z = z_c = \frac{p_{ro}}{1-p_{ro}}$$

for orifice and capillary restrictors, respectively. Analytical solution to the system of equations (9) is easily accomplished(see Davies and Leonard, 1969). The resulting dynamic recess pressures are equal to

$$p_{r\alpha}^{\,n} = -\frac{\dfrac{3p_{ro}}{\delta\theta}\displaystyle\int_{\theta_n}^{\theta_{n+1}} h_\alpha\, d\theta + 12\,\frac{L\Delta\xi}{D\delta\theta}\left[\frac{\Lambda}{2} h_\alpha \Big|_{\theta_n}^{\theta_{n+1}} + i\,\sigma \displaystyle\int_{\theta_n}^{\theta_{n+1}} h_\alpha\, d\theta\right]}{[\,z+1+2\gamma \sin^2(\pi/N)]\,(1+i\,f)} \qquad (10)$$

$$\alpha = x,y;\ n=1,2,..N$$

where $f=\omega/\omega_B$ is a frequency ratio. ω_B is named a "break" frequency, and its relevance on the bearing dynamic force response will be discussed latter. The break frequency is given by the expression:

$$\omega_B = \frac{\pi D c^3}{3N(L-l)\mu\beta V_r}\,(z+1+2\gamma\sin^2(\pi/N)) \qquad (11)$$

Dynamic force coefficients are calculated by integration of the first order pressure field over the journal surface,

$$\frac{K_{\alpha\beta} + i\omega C_{\alpha\beta}}{LD(P_s-P_a)/c} = -\frac{D}{L}\int_0^{L/D}\int_0^{2\pi} p_\beta\, h_\alpha\, d\theta\, d\xi \qquad (12)$$

$$\alpha,\ \beta = x,\ y$$

and it is recalled that $h_x=\cos\theta$ and $h_y=\sin\theta$, respectively. After some algebraic manipulations, it is found that the stiffness and damping coefficients are given by

$$K_{xx} = K_{yy} = K_{xxo}\,\frac{(1+f^2/\alpha_c)}{1+f^2} \qquad (13a)$$

$$C_{xx} = C_{yy} = C_{xxo}\,\frac{(1-\alpha_c)}{1+f^2} \qquad (13b)$$

$$K_{xy} = -K_{yx} = \frac{K_{xyo}}{1+f^2} \qquad (13c)$$

$$C_{xy} = -C_{yx} = -\frac{K_{xyo}}{\omega_B(1+f^2)} \qquad (13d)$$

where K_{xxo}, C_{xxo}, K_{xyo} are the dynamic force coefficients in the absence of the fluid compressibility effect. These coefficients are identical to those presented by Rowe (1980) and presented in Table 1.

The parameter α_c is denoted as a reduced damping factor due to compressibility at zero frequency and given by

$$\alpha_c = \frac{3\ N\ V_r\ (P_r - P_a)\ \beta}{\pi L D c\ [z+1+2\gamma \sin^2(\pi/N)]} \qquad (14)$$

The dynamic force coefficients given in equations (13) depend strongly on the frequency ratio $f=\omega/\omega_B$. Dynamic operation at f=1 results in a reduction of 50% in direct damping and a considerable increase in hydrostatic stiffness. The "break" frequency ω_B, equation (12), is rewritten in terms of the restrictor characteristics as

a) orifice HJB:

$$\omega_B = \frac{A_o\ v_{so}^2}{V_r\ v_o\ z_o} (z_o+1+2\gamma \sin^2(\pi/N)) \qquad (15a)$$

b) capillary HJB:

$$\omega_B = \frac{A_c\ v_{sc}}{V_r\ z_c} (z_c+1+2\gamma \sin^2(\pi/N)) \qquad (15b)$$

where v_s is the fluid velocity at sonic conditions across the orifice or capillar, and v_o is the fluid speed through the orifice restrictor. Appropriate design of HJBs requires the bearing to operate under dynamic conditions well below the break frequency ω_B. As a rule of thumb, it is suggested that operation above f=0.01 should be avoided. High break frequencies can only be achieved on HJBs with shallow recesses (small overall recess plus supply line volumes) and large diameters for the orifice and capillars. For orifice compensated HJBs, a large ratio of sonic speed to fluid orifice speed is desired; while for capillar HJBs, the restrictor length should be kept to a minimum. Of course a negligible value of the fluid compressibility factor β is sufficient to insure adequate dynamic operation without stiffness hardening and reduced damping. It is mentioned that fluids of large viscosity and HJBs with small axial recess lengths are more likely to present low values of the break frequency ω_B.

Dynamic operation at very high frequencies determines a complete loss of damping while the hydrostatic stiffness attains its limiting value. As $\omega \to \infty$, from equation (13a) we obtain

$$K_{xx} \to K_{xx\infty} = \frac{K_{xxo}}{\alpha_c} = \omega_B\ C_{xxo} = N \sin^2(\pi/N)\ \frac{(L+1)\ LR^2}{V_r\ \beta} \qquad (16)$$

Note that the asymptotic value of direct stiffness depends solely on the

compressibility factor β and the recess volume, and it is independent of the fluid properties or external supply conditions.

Although dynamic operation at frequencies well below ω_B is highly desired, the possibility of "pneumatic hammer instability" in a HJB should be carefully analyzed. This phenomenon characteristic of highly compressible fluids such as in gas-lubricated hydrostatic bearings (Lund, 1965) occurs at low frequencies and determines negative values of the direct damping coefficients. At zero frequency, from equation (12b), the value of direct damping is given as $C_{xx} = C_{xxo}\ (1-\alpha_c)$. Thus, null or negative damping is avoided if the reduced damping factor is small, $\alpha_c << 1$, or from equation (14), if

$$\frac{N\ V_r\ (P_r-P_a)\ \beta}{\pi\ LDc} << \frac{1}{3}\left[z+1+2\gamma\ \sin^2(\pi/N)\right] \qquad (17)$$

which requires a low ratio of recess volume to film land volume, and small products of recess pressure and compressibility factor β. This condition possesses a severe restriction on the recess volume and the maximum allowed recess pressure for highly compressible fluids such as liquid hydrogen. Redecliff and Vohr (1969) have recommended that the total volume in the feeding recesses be less than 5% the total volume in the bearing film in order to avoid pneumatic hammer effects. The relation derived in the present analysis gives a better though more stringent criteria. Equation (17) requires the recess volume to be low, and thus, the recess depth must be kept to a minimum consistent with providing uniformity of pressure over the recess.

For hybrid operation, the whirl frequency ratio is a fundamental property of the bearing(independent of the rotor system) which determines the maximum shaft operating speed before whirl instability occurs. The whirl ratio ϕ is defined as

$$\phi = \frac{K_{xy}}{\Omega\ C_{xx}} = \frac{1}{2\ (1-\alpha_c)} \qquad (18)$$

Thus, in a centered HJB the whirl ratio ϕ is at most equal to 0.50, and it is substantially increased if the reduced damping factor α_c is large. From a rotordynamics point of view, hybrid bearings offer no advantage in relation to plain journal bearings. Additionally, if fluid recess compressibility is large, it causes the limited applicability of hybrid bearings to be further restricted.

The conditions stated are of considerable importance in HJBs used for cryogenic applications such as those handling liquid hydrogen. For LH2, the compressibility factor β is rather large while its viscosity is very small. Typical bearing supply pressures exceed 6.9MPa(1000 psig) in order to attain the required levels of load capacity. In this case, even if recesses of low depth are designed, it is very likely that the reduction in damping due to the fluid compressibility is large.

EXAMPLES

The following sample case serves to show the effect of recess compressibility on the dynamic force coefficients of a typical capillary HJB.

The example has been taken from an application presented by Rhode(1976). The geometric and operating parameters for the bearing are as follows:

N=8, L=35.56 mm(1.4in), D=71.12 mm(2.8in),
l=30.48 mm(1.2in), b=22.84 mm(0.9in),
c=0.0254mm(0.001in), Hr/c=10,30,50,
d_c=0.325mm, l_c=19.1mm,

μ=0.0345 Ns/m^2, β=5.8 10^{-10} m^2/N,

P_s-P_a = 689.5 KPa(1000 psig), p_{ro}=0.3
Ω= 1000 rpm (16.66 Hz),

For the sample bearing, the static direct stiffness and damping coefficients at zero frequency and no compressibility are equal to K_{xxo}=5.20 10^7 N/m and C_{xxo}=2.5 10^6 Ns/m, respectively. For 3 different values of the recess depth, Figures 2 and 3 show the variation of K_{xx} and C_{xx} for increasing values of the frequency ratio f. The calculated values of the break frequency and reduced damping factor are given by

Hr/c=10; λ_2=0.0044, ω_B=2281 Hz, α_c=0.001448,
Hr/c=30; λ_2=0.0124, ω_B= 809 Hz, α_c=0.004081,
Hr/c=50; λ_2=0.0204, ω_B= 492 Hz, α_c=0.006710,

Figure 2 shows that the direct stiffness increases dramatically as the excitation frequency grows. Note that the greater the break frequency(smaller recess depth), the greater is the asymptotic value of the stiffness coefficient. Figure 3 shows the damping coefficient to decrease as the excitation frequency increases. Note that the damping curves are almost identical due to the smallness of the reduced damping factor α_c. The whirl frequency ratio for synchronous excitation at 1000 rpm is very close to 0.5 due to the smallness of the factor α_c. No significant reduction in damping is found at low frequencies due to the low product of recess pressure and compressibility parameter β.

The effect of a large compressibility factor β on a shallow recess, orifice compensated HJB has been considered. The sample bearing is typical of a current cryogenic application with liquid hydrogen as the working fluid. The geometric and operational parameters for the bearing are given as follows:

N=8, L=62.58mm(2.463in), D=84.43 mm(3.32in),
l=b=22.776mm(0.896mm)
c=0.0254mm(0.001in), Hr/c=5,10,15
d_o=0.779mm,

μ=6.279 10^{-6} Ns/m^2, ρ=51.11 kg/m3, β=8.86 10^{-9} m^2/N,

P_s-P_a = 20.684 MPa (3000 psig), p_{ro}=0.5

Ω = 25000 rpm (416.6 Hz)

The operating parameters determine the flow regime in the bearing to be turbulent, and thus, the results of the present analysis are not valid. However, the author (SanAndres,1989a) has presented a similar analysis for turbulent HJBs

with inertia effects. This analysis is more complex and does not provide closed form formulae for direct evidence of the compressibility effect on the dynamic force coefficients.

Figures 4 and 5 show the synchronous ($\omega=\Omega$) stiffness and damping coefficients for increasing recess depths and as a function of the compressibility parameter β. For the value of β corresponding to liquid hydrogen, the calculated break frequency ω_B is well above 10^3 Hz and thus, fluid compressibility does not affect greatly the direct stiffness coefficients. Figure 2 shows the stiffness coefficients to be constant since essentially the frequency ratio f is almost zero for the application considered. Figure 5 shows the direct damping coefficient to be greatly affected by the compressibility parameter β and the recess depth. The loss in damping at the operation point for LH2 is larger for the largest recess depth considered.

Figure 6 shows the whirl frequency ratio ϕ to approach a value equal to 0.5 as the compressibility parameter tends to zero(incompressible, $\beta \rightarrow 0$). As β increases, the whirl ratio ϕ also increases denoting a substantial reduction in available direct damping. At a value of $\beta=8.88\ 10^{-8}$ m^2/N typical for LH2, the whirl ratio ϕ raises from 0.554 to 0.651 as the recess depth increases from 5 to 15 times the bearing clearance.

The results presented clearly show the inconvenience of the proposed HJB since the stability characteristics of the bearing are worse than those of a plain journal bearing. Further reduction of the recess depth will certainly reduce the whirl frequency ratio but will convert the HJB into a plain journal bearing and cause a drastic reduction in direct hydrostatic stiffness. Suggested fixes that can substantially improve the stability characteristics of the bearing are

a) to reduce the axial extent of the recess so as to reduce the recess volume and provide more space for development of the squeeze film damping effect. However, shorter recess axial lengths will determine reduced hydrostatic stiffness. To reduce the recess circumferential extent is not recommended since then the mean flow circumferential velocity will grow rapidly and it may determine and effective increase in the whirl ratio.

b) A roughened bearing surface will reduce substantially the cross coupled stiffness coefficient and reduce the whirl ratio ϕ well below 0.5 (SanAndres, 1989b). Fluid injection opposite to shaft rotation may also reduce the cross-coupled effects, although a quantitative analysis is not yet available.

CONCLUSIONS

The dynamic behavior of externally pressurized bearings has been shown to be highly dependent on the fluid compressibility at the bearing recesses. At high frequency excitations beyond a break frequency, the bearing hydrostatic stiffness increases sharply and it is accompanied by a rapid decrease in direct damping. Also, the potential of pneumatic hammer instability (negative damping) at low frequencies seems to be certain in hydrostatic bearing applications handling highly compressible fluids.

The analysis presented has shown that the bearing dynamic force response

for the entire frequency spectrum is determined by just 2 parameters, the break frequency ω_B and the reduced damping factor α_c. Criteria to avoid stiffness hardening and damping reduction by removing the break frequency well above the desired operating frequency are derived and discussed. At low frequencies, the dynamic performance of the bearing is substantially degraded if the reduced damping factor is large. Furthermore, the limited stability characteristics of hybrid bearings are severely restricted. To avoid this effect it is required for the recess volumes(recess depth) to be small. However, for highly compressible fluids, improved bearing stability characteristics may demand a reduced limit on the maximum external supply pressure to the bearing. Consequently, reduced load capacity and stiffness are to be traded off for stability. HJBs with a roughened bearing surface could be an appropriate alternative for better bearing stability and dynamic performance.

REFERENCES

Davies, P.B., and Leonard, R., 1969, "The Dynamic Behavior of Multi-Recess Hydrostatic Journal Bearings," Proc. Instn. Mech. Engnrs., Vol. 184, Part 3L, pp. 139-144.

Davies, P.B., and Leonard R., 1970, "Stability of Multirecess Hydrostatic Journal Bearings," Journal of Mechanical Engineering Science, Vol. 12, 2, pp. 150-152.

Ghosh, M.K. , Majumdar B.C., and J.S. Rao, 1979, "Steady State and Dynamic Behavior of Multirecess Hybrid Journal Bearings," Journal of Mechanical Engineering Science, Vol. 21, 5, pp. 345-351.

Ghosh, M.K, and N.S. Viswanath, 1987, "Recess Volume Fluid Compressibility Effect on the Dynamic Characteristics of Multirecess Hydrostatic Journal Bearings," ASME Journal of Tribology, Vol. 109, pp. 417-426.

Ghosh, M.K., S.K. Guha, and B.C. Majumdar, 1989, "Rotordynamic Coefficients of Multirecess Hybrid Journal Bearings," WEAR, Vol. 129, pp. 245-259.

Leonard, R., and W.B. Rowe, 1973, "Dynamic Force Coefficients and the Mechanism of Instability in Hydrostatic Journal Bearings," WEAR, Vol. 23, pp. 277-282.

Lund, J.W., 1965, "A Theoretical Analysis of Whirl Instability and Pneumatic Hammer for a Rigid Rotor in Pressurized Gas Journal Bearings," ASME Paper 65-Lub-12.

Redecliff, J.M., and J.H. Vohr, 1969, "Hydrostatic Bearings for Cryogenic Rocket Engine Pumps," ASME Journal of Lubrication Technology, pp. 557-575.

Rhode, S.M., and H.A. Ezzat, 1976, "On the Dynamic Behavior of Hybrid Journal Bearings," ASME Journal of Lubrication Technology, pp. 557-575.

Rowe, W.B., 1980, "Dynamic and Static Properties of Recessed Hydrostatic Journal Bearings by Small Displacement Analysis," ASME Journal of Lubrication Technology, Vol. 102, pp. 71-79.

San Andres, L.A., 1989a, "Approximate Analysis of Turbulent Hybrid Bearings. Static and Dynamic performance for Centered Operation," submitted for review to

ASME Journal of Tribology.

San Andres L.A., 1989b, "Turbulent Hybrid Bearings with Fluid Inertia Effects, I-Analysis and Numerical Model, II-Results and Discussion," submitted for review to ASME Journal of Tribology.

Singh, D.V., R. Sinhasan, and R.C. Ghai, 1979, "Static and Dynamic Characteristics of an Orifice Compensated Hydrostatic Journal Bearing," ASLE Transactions, Vol. 22, 2, pp. 162-170.

TABLE 1

Dynamic Force Coefficients for Laminar Flow Hydrostatic Journal Bearings

no fluid compressibility effects

$$K_{xxo} = K_{yyo} = \frac{3N^2}{4\pi} \sin^2(\pi/N) \frac{(1 + 1/L)}{(z+1+2\gamma\sin^2(\pi/N))} p_{ro} \frac{(P_s - P_a)LD}{c}$$

$$C_{xxo} = C_{yyo} = \frac{3N^2}{4\pi} \sin^2(\pi/N) \frac{(1 + 1/L)(1 - 1/L)}{(z+1+2\gamma\sin^2(\pi/N))} \frac{\mu L^3 D}{c^3}$$

$$K_{yxo} = -K_{xyo} = \frac{3N^2}{8\pi} \sin^2(\pi/N) \frac{(1 + 1/L)(1 - 1/L)}{(z+1+2\gamma\sin^2(\pi/N))} \frac{\mu\Omega L^3 D}{c^3}$$

$$C_{yxo} = C_{xyo} = 0$$

where $z_o = \frac{p_{ro}}{2(1-p_{ro})}$; $z_c = \frac{p_{ro}}{1-p_{ro}}$

$$\gamma = \frac{2\,\Delta\xi\, L}{\delta\theta\,\Delta\theta\, D}$$

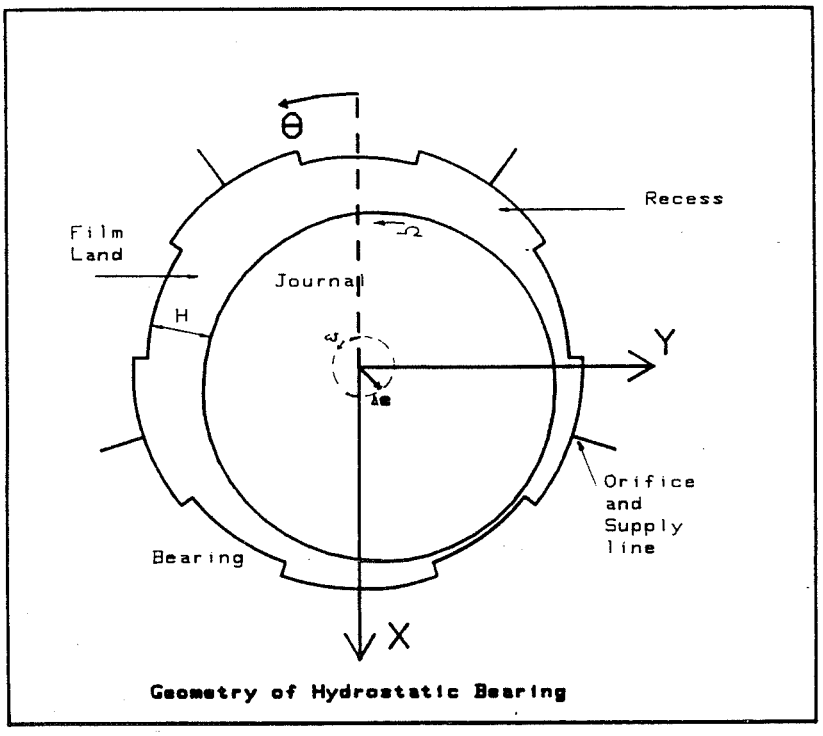

Figure 1. Geometry of a hydrostatic journal bearing and description of coordinate systems.

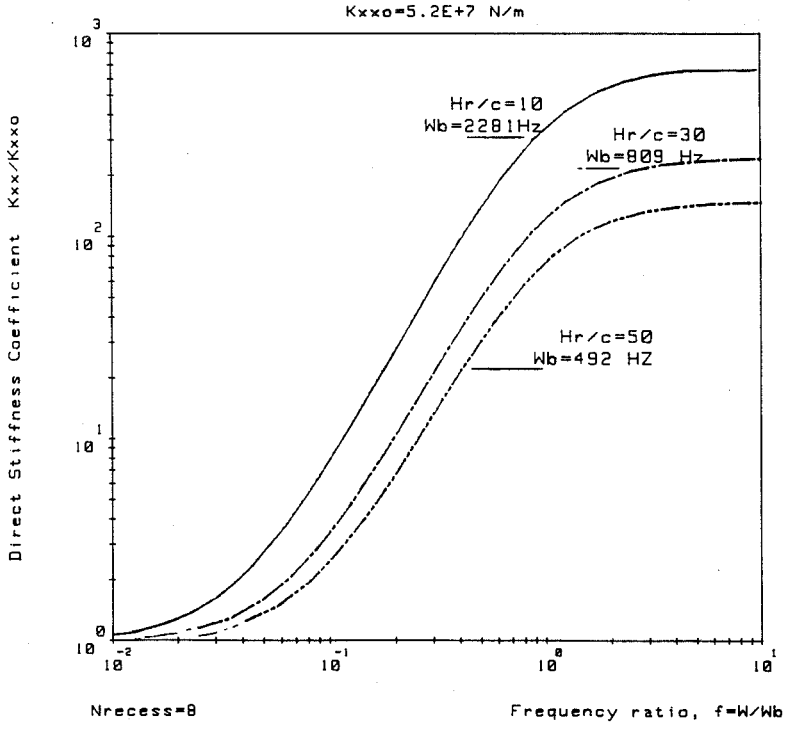

Capillar HJB: L/D=.5, 1000rpm, Ps=689500Pa, c=2.54E-5m

Figure 2. Effect of excitation frequency on direct stiffness for a capillary hydrostatic journal bearing with increasing recess depths.

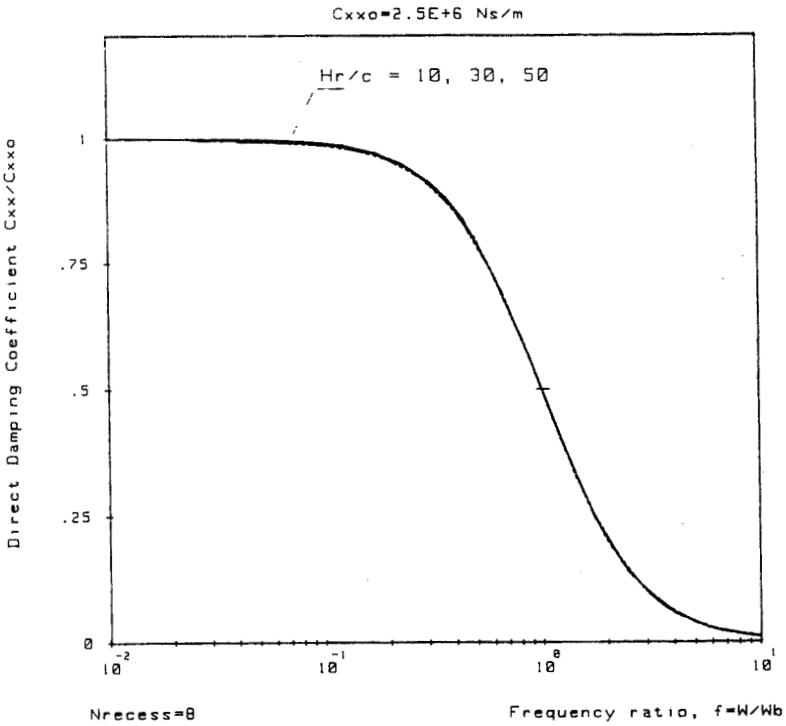

Figure 3. Effect of excitation frequency on direct damping for a capillary hydrostatic journal bearing with increasing recess depths.

Capillar HJB: L/D=.5, 1000rpm, Ps=689500Pa, c=2.54E-5m

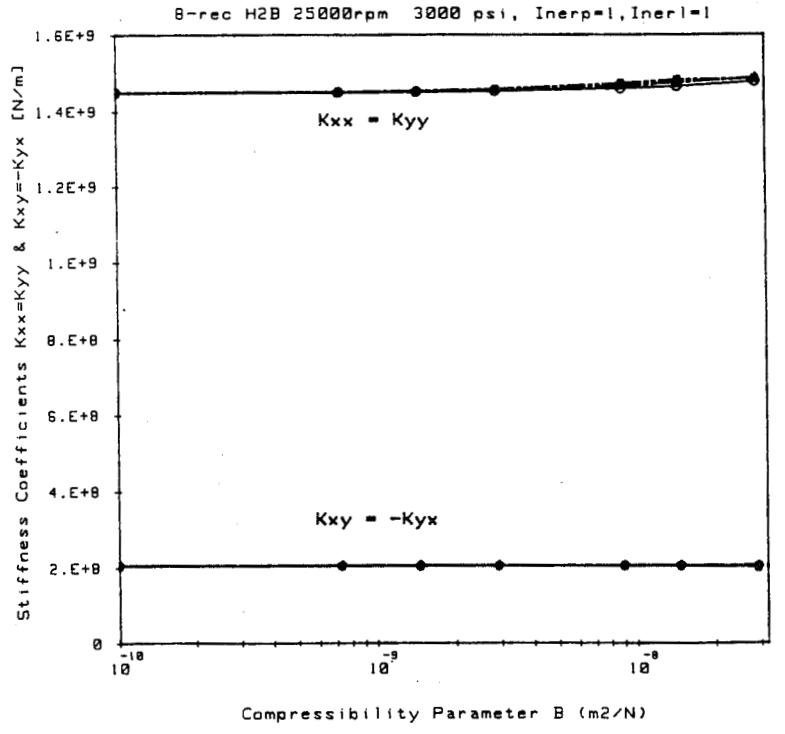

ω=Rpm=25000; c=2.54E-5m, Hr/c=5,10,15, l=22.7mm

Figure 4. Effect of fluid compressibility factor β and recess depth on synchronous stiffness coefficients for a liquid hydrogen, orifice compensated, hybrid bearing.

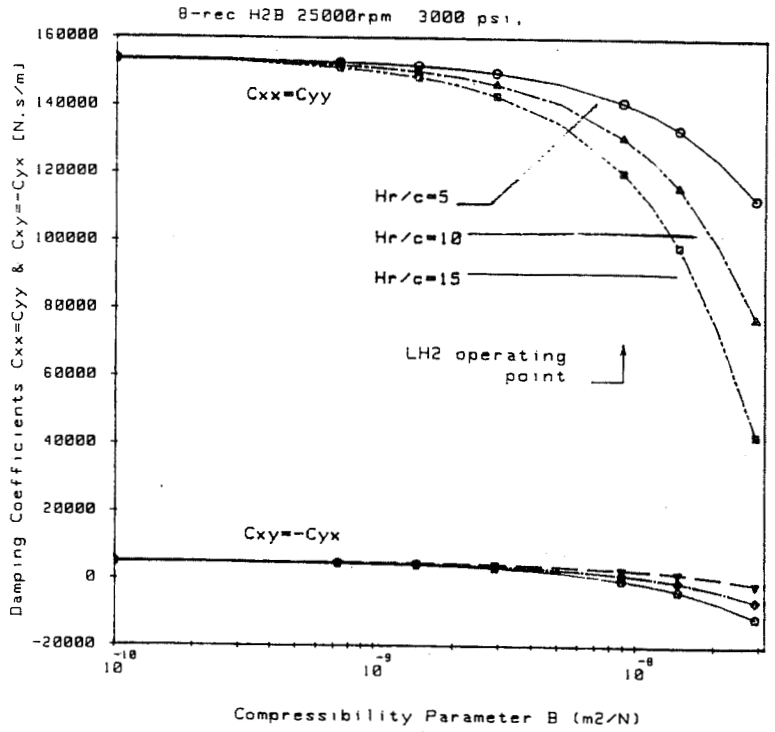

w=rpm=25000; c=2.54E-5m, Hr/c=5,10,15; l=22.7mm

Figure 5. Effect of fluid compressibility factor β and recess depth on the synchronous damping coefficients for a liquid hydrogen, orifice compensated, hybrid bearing,

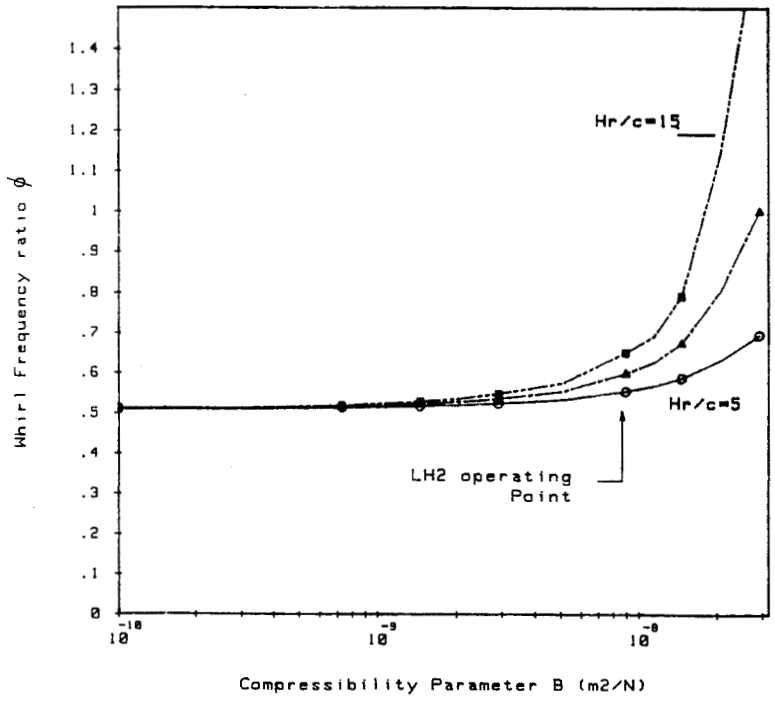

w=Rpm=25000; c=2.54E-5m, Hr/c=5,10,15, l=22.7mm

Figure 6. Whirl Frequency ratio ϕ for a LH2 hybrid bearing. Combined effect of fluid compressibility and recess depth.